



Application possibilities and chemical origin of sub-micrometer adhesion modulation on polymer gratings produced by UV laser illumination

M. Csete ^{a,*}, G. Kurdi ^a, J. Kokavecz ^a, V. Megyesi ^a, K. Osvay ^a, Z. Schay ^b, Zs. Bor ^a, O. Marti ^c

^a Department of Optics and Quantum Electronics, University of Szeged, Dóm tér 9, 6720 Szeged, Hungary

^b Department of Surface Chemistry and Catalysis, Chemical Research Centre, Konkoly Thege M. út 29-33, 1121 Budapest, Hungary

^c Department of Experimental Physics, University of Ulm, Albert Einstein Allee 11, 89069 Ulm, Germany

Abstract

Sub-micrometer periodic structures were prepared on the surface of poly-carbonate films by UV laser treatment methods: a) grating-like structures having a period of 156 nm were induced by ArF excimer laser, b) 416 nm and 833 nm periodic gratings were prepared by two-beam interference realized by the fourth harmonic of a Nd:Yag laser. The sub-micrometer adhesion pattern accompanying the topographical structure was determined by pulsed force mode atomic force microscopy. The difference between the measured adhesion modulation and the adhesion profile calculated based on the topography was explained by the UV laser illumination caused phase and chemical changes. XPS investigations proved that chemical modification of the polymer occurs and the degree of the photo-degradation depends on the treating laser wavelength as well as on the number and fluence of the laser pulses. It was demonstrated by tapping mode atomic force microscopy that bovine serum albumin attaches to surface parts having higher adhesion. The dependence of the protein adherence on the surface treatment conditions was demonstrated based on the C 1s and O 1s spectra and on the proteinaceous nitrogen level.

© 2005 Elsevier B.V. All rights reserved.

Keywords: Sub-micrometer polymer grating; Atomic force microscopy; Adhesion; Protein adherence

1. Introduction

A survey of the literature proves that polymeric materials are widely applied for immobilization of biological cells and macromolecules [1]. In biomedical investigations the adsorption of serum proteins by an appropriate polymeric substrate is a precursor step in cell culture formation [2]. New important challenges appeared in the field of biosensor development devoted to improve the sensitivity and specificity of the diagnostic methods, where polymeric surfaces having unique properties may open new possibilities [3].

The intact polymer surfaces are usually hydrophobic caused by their low surface energy, which is a barrier to these applications. Different treatment methods are capable of modifying the physical properties and chemical composition of the surface layer in order to improve the fluid wettability, adhesive bonding and biocompatibility. The effect of the nanoscale topography on the hydrophobicity was

proven by dynamic contact angle measurements on fluoro-based polymer films spin-coated onto pre-structured layers having different surface profiles [4]. The possibility to increase the hydrophilicity by UV lamp illumination and by the exposure to ozone atmosphere was shown in case of originally non-polar polymers. The origin of the polarity enhancement is that the treated surface layer is rich in oxygen and contains the remnants of the chain scission [5]. The oxidation and photo-degradation manifests itself in specific micro-mechanical changes demonstrated by friction force atomic force microscopy and nano-indentation measurements [5,6].

The UV laser based surface treatment results in combined modification of the topography, the micromechanical and chemical properties caused by the laser illumination induced thermal and chemical processes [7]. The advantage of the application of laser illumination is the available sub-micrometer resolution and the possibility to control the contribution of topographical and chemical effects by changing the experimental conditions.

In our present study we utilized UV laser treatment techniques to prepare periodic structures on poly-carbonate

* Corresponding author. Tel.: +36 62 544 420; fax: +36 63 544 658.

E-mail address: mcsete@physx.u-szeged.hu (M. Csete).

(PC) surfaces. The resulted topographical and adhesion pattern was studied by Pulsed Force Mode (PFM) Atomic Force Microscopy (AFM) with sub-micrometer resolution. XPS measurements were performed to identify the UV laser induced chemical changes. We investigated the adherence of bovine serum albumin (BSA) by Tapping Mode (TM) AFM on different structures with the purpose to analyze, how the adhesion modulation originated from the topography and chemical heterogeneity influence the protein distribution.

2. Experimental

2.1. Polymer-film preparation and protein adherence procedure

Thin poly-carbonate films were prepared by dissolving PC grains (Bayer, MW: 24.000) in chloroform and spin-coating drops from the solutions having 10 mg/ml concentration at 2500 rotation/min speed of spinning onto freshly cleaned silicon wafers. The protein seeding was performed applying the procedure described in Ref. [8]. One 50 μ l drop from BSA solutions having a concentration of 100 μ g/ml was put on intact and laser treated PC layers.

2.2. Laser induced periodic surface structure generation

The illumination of solid surfaces by polarized laser beam having a fluence below the material damage threshold results in Laser Induced Periodic Surface Structure formation. The LIPSS originate from scattered beam interference as it was proven based on the dependence of the structure's period on the wavelength and angle of incidence. The inhomogeneous intensity distribution induces self-organized processes leading to grating-like structure development [9]. In our present study we selected the most homogeneous part of the ArF excimer laser beam, and realized linear polarization by one thin-layer polarizer (Laseroptik GMBH). The fluence of the beam was adjusted to $F_{av}=4$ mJ/cm² by an attenuator module (Optec), and LIPSS was generated by several thousands of laser pulses (Fig. 1a).

2.3. Grating generation by two-beam interference

Different methods are described in the literature which makes it possible to realize the two-beam interference based on the application of a beam-splitter, prism or grating as a splitting device [10–12]. The low entire energy transferred in the case of grating-based method is determined by the diffraction efficiency and is limited by the damage threshold of the master grating. Only in the case of polymeric materials is it possible to convert the periodic interference pattern into surface structures via laser induced melting and ablation thanks to the low threshold fluences.

We illuminated different master gratings (Spectrogon, PUV, 600 and 1200 lines/mm) by the fourth harmonic of a Nd:Yag laser ($\lambda_{FH}=266$ nm) in the experimental arrangement presented in Fig. 1b. The diffraction efficiency was 30% for both

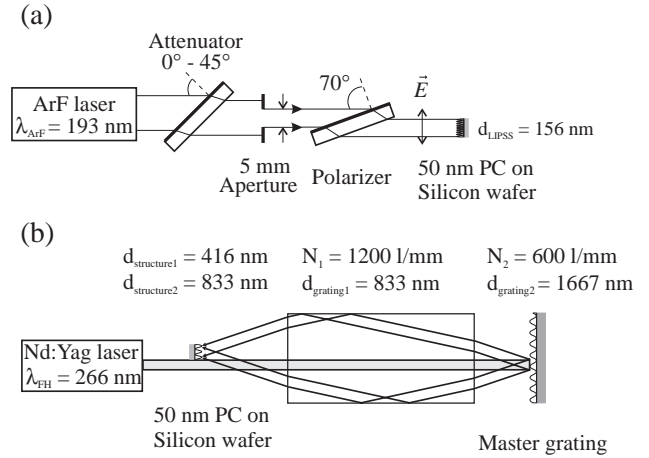


Fig. 1. (a) The experimental setup applied to generate LIPSS by linearly polarized ArF excimer laser beam. (b) The experimental arrangement applied to realize the two-beam interference by the fourth harmonic of a Nd:YAG laser.

of the first order diffracted beams and the average fluence of the combined beams was tuned in the region of $F_{av}=5.2–10.4$ mJ/cm² by rotating a half-wave plate after the frequency doubling.

2.4. Pulsed force mode and tapping mode atomic force microscopy

Pulsed Force Mode AFM (WITec GmbH) was applied to study the topography and the adhesion on the UV laser treated surfaces [13]. The sine voltage modulation of the Z piezo-tube having an optimal frequency and amplitude determined by the tip-sample parameters lead the tip to jump in and out of contact in each cycle. The topography and the adhesion are simultaneously determined based on the maximum repulsive and attractive forces, measurable at the tip, that are approaching to and receding from the surface, respectively. We calibrated the k [nN/nm] spring constant of the tips (Nano-sensors FMR 22742) by Sader-method [14]. The adhesion signal was converted into force based on the following equation:

$$F_{adh}[nN] = F_{adh}[V] \cdot \frac{1}{P} \cdot \frac{1}{S[nA/nm]} \cdot k[nN/nm] \cdot C \quad (1)$$

where $F_{adh}[V]$ is the signal measured at the maximal cantilever deflection, P is an optional gain of the instrument and C is a constant determined by the signal collecting electronics. The S [nA/nm] sensor response was established by calibration using a built in routine.

PSIA AFM operating in tapping mode was applied to analyze the BSA adherence on different laser treated surfaces. It is known from the literature that the phase signal is affected also by the topography, but in case of chemically heterogeneous surfaces the adhesion, the visco-elasticity and the charge distribution cause additional phase changes [15]. Based on this the phase can be used as material-dependent signal complementary to the topography [16]. Tapping AFM tips (NT-MDT NSG11) having a spring

constant of 5.5 N/m and resonance frequency of 150 kHz were applied, the typical tip radius was larger than in the case of PFM tips resulting in smaller contrast. The amplitude of the tip-oscillation was calculated according to the manual of the device.

2.5. XPS analysis

We performed XPS measurements on the intact polymer surfaces, and on the treated surface areas comprising LIPSS

and gratings generated by the two-beam interference. Further XPS studies were realized to demonstrate the presence of the albumin and the dependence of the protein adherence on the experimental conditions. The XP spectra were collected by a KRATOS XSAM 800 machine using MgK α radiation with 120 W power and FAT mode with 40 eV pass energy. The silicon wafers were cut to about 10 \times 10 mm size and fixed to the sample holder by double sided carbon adhesive tape. The electrostatic charging of the sample was about 2 eV. The C 1s line at 285 eV binding energy was used for charge referencing.

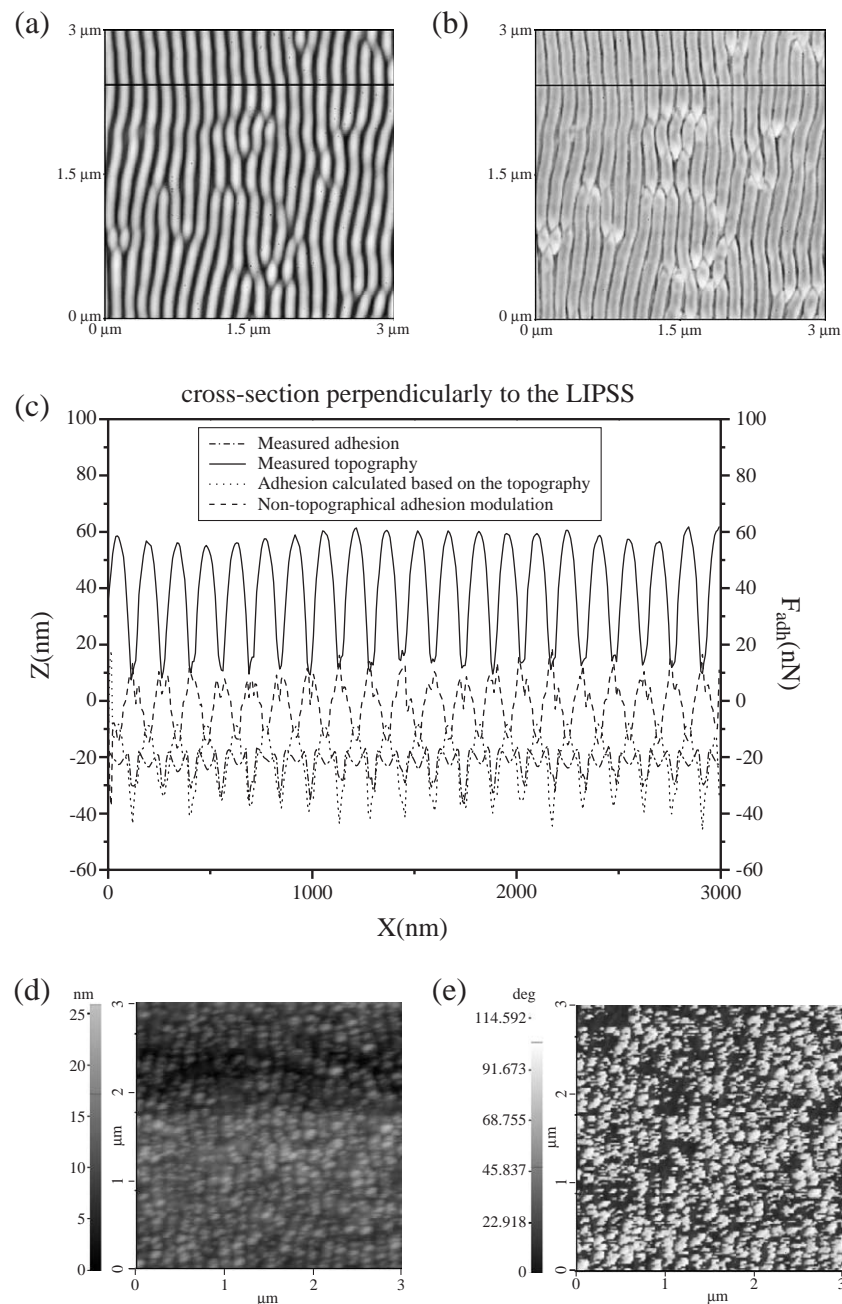


Fig. 2. Laser induced periodic surface structure having a period of $d_{\text{LIPSS}} = 156$ nm, generated by 1000 polarized ArF laser pulses having a fluence of $F_{\text{av}} = 4$ mJ/cm 2 : (a) topography; (b) adhesion; (c) comparison of the measured and calculated adhesion modulation along the line cross-section taken perpendicularly to the structure, indicated on (a)–(b); (d) topography; and (e) phase image after BSA adherence. Bright areas in phase image correspond to the protein islands adhered at the top of the hills.

The data were evaluated by the VISION software supplied by KRATOS.

3. Results and discussion

3.1. The topography and adhesion measured on surfaces comprising LIPSS and gratings generated by the two-beam interference

The repeated illumination of poly-carbonate surfaces by polarized ArF excimer laser beam caused grating-like structure development (Fig. 2a). The period of these structures corre-

sponds to the intensity distribution determined by scattered-beam interference:

$$d_{LIPSS} = \frac{\lambda}{n_{selvedge} - \sin\alpha} \tag{2}$$

where $d_{LIPSS}=156$ nm is the period of the LIPSS at $\alpha=0^\circ$ angle of incidence, and $n_{selvedge}=1.33$ is the index of refraction of the light modified thin upper polymer layer [9]. The PFM AFM measurements have shown sub-micrometer adhesion modulation. The peculiarity of this modulation is that the adhesion is increased at the hills and decreased at the valleys,

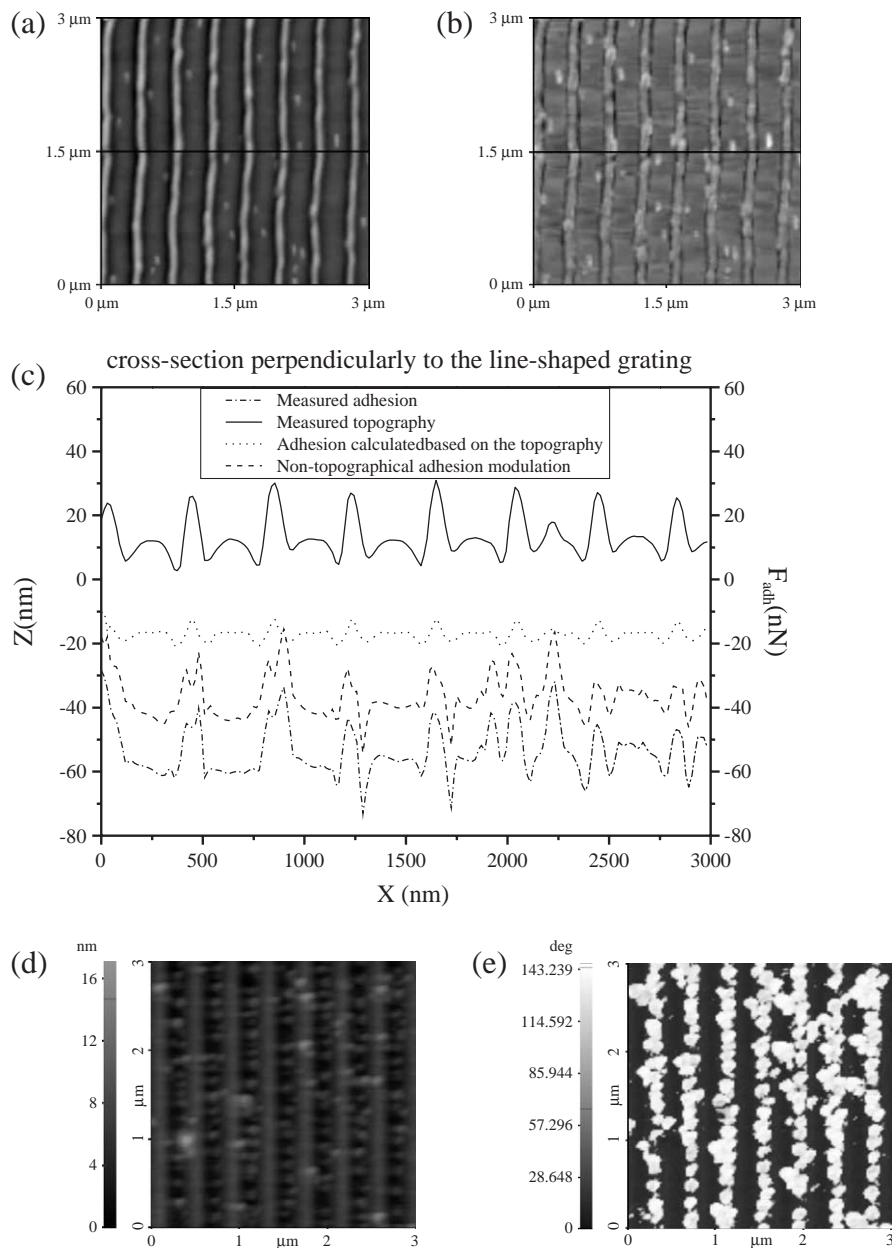


Fig. 3. Line-shaped two-beam interference grating having a period of $d_{structure1}=416$ nm generated by 500 “s” polarized laser pulses of the fourth harmonic of a Nd:YAG laser having a fluence of $F_{av}=7.28$ mJ/cm²: (a) topography; (b) adhesion; (c) comparison of the measured and calculated adhesion modulation along the line cross-section taken perpendicularly to the grating grooves, indicated on (a)–(b); (d) topography; and (e) phase image after BSA adherence. Bright areas in phase image signify the protein islands adhered in the valleys.

which is reversed compared to changes caused by the topography (Fig. 2b–c).

The two-beam interference realized by the fourth harmonic of the Nd:Yag laser resulted in an intensity distribution at the target plane:

$$I(x) = I_{\text{average}} \left(1 + V \cdot \cos \left(\frac{2\pi x}{d_{\text{structure}}} \right) \right) \quad (3)$$

where I_{average} and $I(x)$ are the average and place dependent intensities, V is the visibility of the interference fringes, $d_{\text{structure}1}=416$ nm and $d_{\text{structure}2}=833$ nm are the periods of the interference fringes in case of 1200 lines/mm and 600 lines/mm master gratings, respectively. The period of the dominant structure developing after illumination by several hundreds of

laser pulses corresponds to the periodicity of this interference pattern. The ratio of the widths of the valleys and hills is determined by the average fluence and the visibility.

The “s” polarized laser beam illumination resulted in the development of gratings built up from continuous polymer stripes (Fig. 3a), while in case of “p” polarized beam the repeated irradiation caused the polymer stripes to divide into droplets. The combined structure comprises both of the two-beam interference originated grating, and the LIPSS-like structure arranged parallel to the direction of the polarization (Fig. 4a).

The adhesion pattern measured perpendicularly to the grating grooves relates to topographical effect (Figs. 3b–c, 4b–c), but the reversed adhesion modulation typical for the

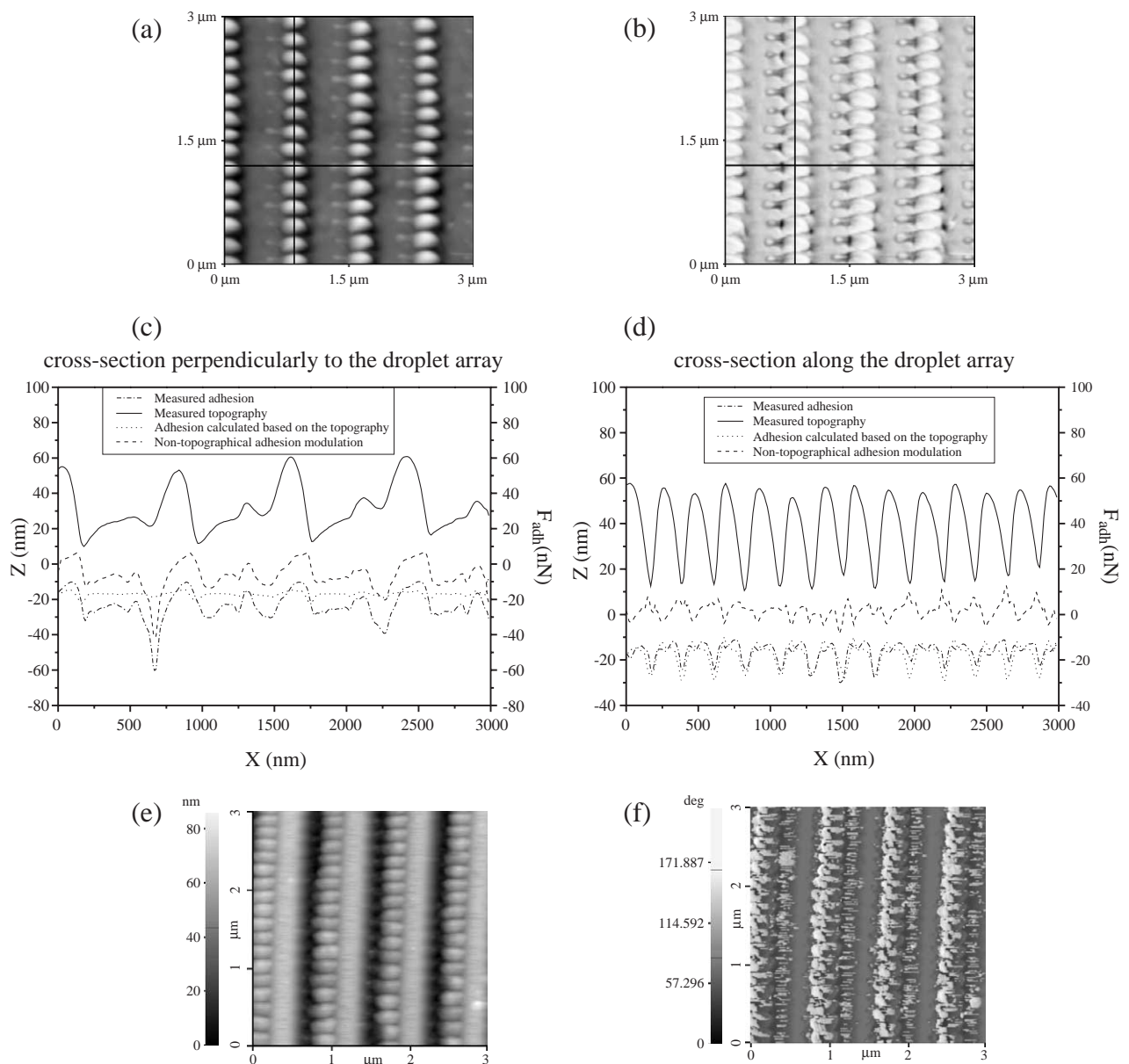


Fig. 4. Two-beam interference droplet grating having a period of $d_{\text{structure}2}=833$ nm generated by 1800 “p” polarized laser pulses of the fourth harmonic of a Nd:YAG laser, having a fluence of $F_{\text{av}}=5.2$ mJ/cm²: (a) topography; (b) adhesion; (c)–(d) comparison of the measured and calculated adhesion modulation along the line cross-sections taken perpendicularly to and along the droplet arrays, indicated on (a)–(b); (e) topography; and (f) phase image after BSA adherence. Bright areas in phase indicate the protein islands adhered in the valleys around the droplets.

LIPSS is also recognizable along the polymer droplet arrays, as it can be seen in Fig. 4b, d. The repeated illumination causes to develop deep valleys around the droplets, and the value of the adhesion is the highest in these valleys.

3.2. Theoretical comparison of the measured adhesion modulation and the effect caused by the periodic topography

We performed numerical calculation to compare the adhesion modulation that originated from the topography and the measured adhesion pattern. The correction of the measured topographical line cross-sections was realized taking into account $R_{tip}^{PFM}=25$ nm radius of curvature of the PFM tip. The adhesion modulation caused by the curvature of the surface profile was calculated based on the Derjaguin–Müller–Toporov (DMT) approximation [17]:

$$F_{adhesion}(R_{surface}^{corrected}) = F_{adhesion}(R_{surface} = \infty) \cdot \frac{R_{tip}^{PFM} \cdot R_{surface}^{corrected}}{R_{tip}^{PFM} + R_{surface}^{corrected}} \quad (4)$$

where $R_{surface}^{corrected}$ is the corrected radius of curvature of the topography, and $F_{adhesion}(R_{surface} = \infty) = 17$ nN adhesion measured on flat poly-carbonate surface was taken into account. The non-topographical adhesion modulation was determined

by subtracting the adhesion calculated along the given line cross-section from the corresponding measured adhesion profile.

In the case of LIPSS there is a well defined reversed adhesion increase at the hills, and decrease in the valleys (Fig. 2c), resulting in double adhesion pattern. Our previous studies have proven that there is no significant material removal at the fluence applied to generate LIPSS formation. The structure development is the result of the material rearrangement during phase changes [7]. The phase transitions and the UV illumination caused chemical changes result in the non-topographical, reversed adhesion modulation.

The analyses of the line profiles taken perpendicularly to the two-beam interference gratings has shown that there is stronger adhesion increase in the valley than the topographical effect (Figs. 3c–4c). The additional reversed adhesion increase is identifiable on the line cross-sections taken along the droplet arrays (Fig. 4d). In case of gratings generated by the two-beam interference both of the material removal and rearrangement play important role. The valleys correspond to the areas illuminated by the highest fluence, and the reminded surface layer suffers stronger degradation, than the polymer stripes or droplet arrays, where the average fluence causes phase and reduced chemical changes like in case of LIPSS formation.

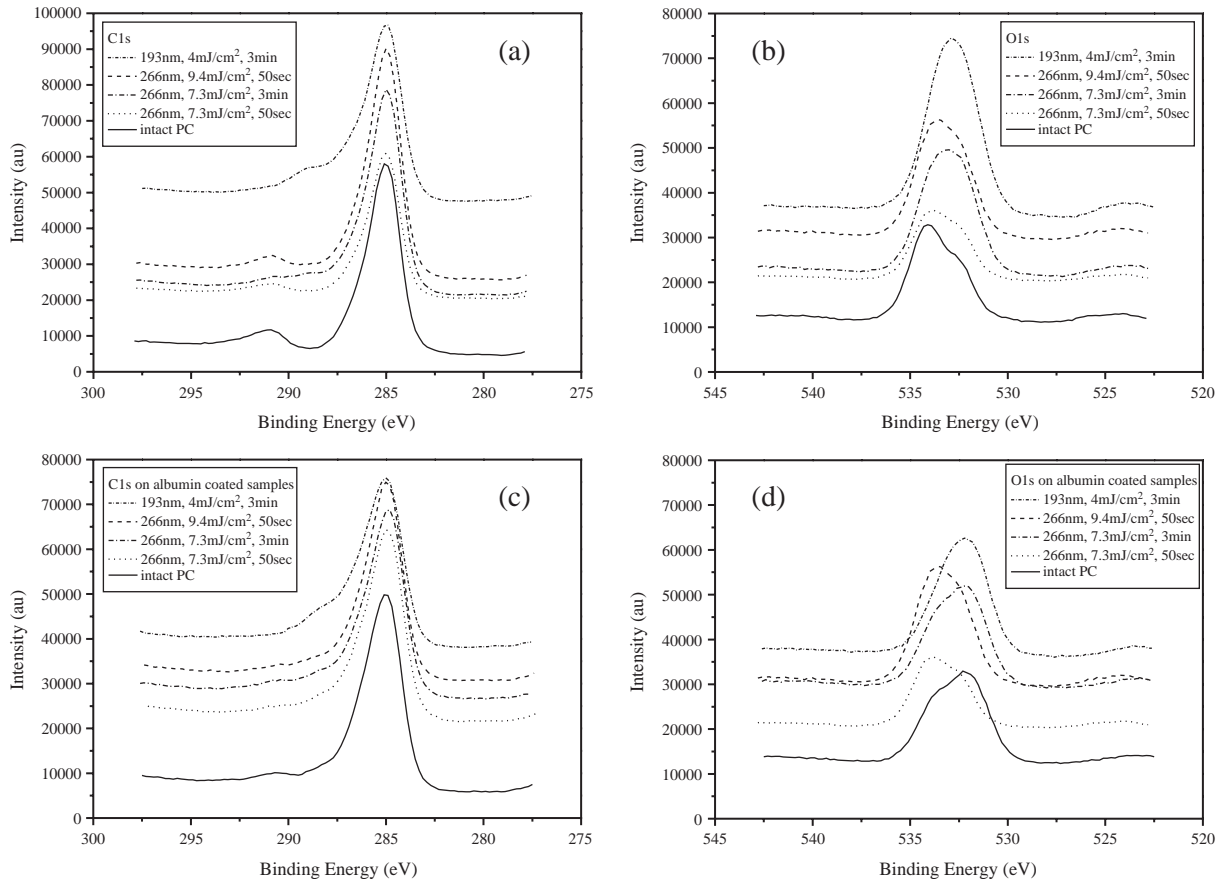


Fig. 5. The dependence of the (a) C 1s; and (b) O 1s XP spectra on the experimental conditions. The influence of the BSA adherence on the (c) C 1s; and (d) O 1s XP spectra.

3.3. Albumin adherence on periodic structures studied by tapping mode AFM

The topography and phase signals about different laser induced gratings were collected before and after BSA seeding. A weak phase modulation was detectable on the laser treated surfaces caused by laser induced chemical heterogeneity. The presence of BSA resulted in very large phase modulation, and the distribution of the protein islands proved that the BSA prefers to adhere onto surface areas where higher adhesion was measured by the hydrophilic AFM tip. The BSA covered the hills of the LIPSS (Fig. 2d, e); the valleys of the line shaped gratings generated by the two-beam interference were filled with the protein aggregates (Fig. 3d, e); while in the case of droplet arrays the BSA was collected around the droplets (Fig. 4e, f).

3.4. Chemical changes of the poly-carbonate caused by UV laser illumination

The comparison of the C 1s and O 1s spectra measured on the intact and laser treated surface parts proved, that the UV laser illumination cause photo-degradation of the poly-carbonate (Fig. 5). The peak appearing at 288–289 eV in the C 1s spectra corresponds to an increase in the amount of C=O bindings and formation of aldehyde and ketone groups. The change in the symmetry of the O 1s spectra refers also to these chemical changes, and a slight increase in the O/C ratio was found. The highest level of photo-degradation was identifiable in the case of the shorter wavelength, and the increase of the number and fluence of laser pulses caused a stronger effect. The detected photo-degradation results in more polar, i.e. more hydrophilic polymer surface. The presence of the attached albumin manifests itself in additional changes in the C 1s and O 1s spectra. The dependence of the proteinaceous nitrogen level on the wavelength, on the number and fluence of the applied laser pulses correlated with the dependence of the degradation level on the experimental conditions. The XPS measurements proved greater extent of protein adherence on surfaces suffered stronger photo-degradation.

4. Conclusions

We prepared grating like-structures by UV laser illumination methods on poly-carbonate surfaces. Pulsed force mode AFM investigation proved the existence of adhesion modulation accompanying the sub-micrometer topographical structures, which is determined by periodically repeating phase and chemical changes. XPS investigation has shown photo-degradation enhancing the polarity of the polymer surface. The places of albumin attachment corresponded to the areas having higher adhesion, and the hydrophilicity-selective

protein adherence resulted in an increase/decrease in the modulation depth of the LIPSS/gratings generated by the two-beam interference, respectively. These results have shown that the UV laser based polymer structuring is promising to develop special sensing surfaces comprising sub-micrometer gratings, which may be utilized in bio-sensorization based on the application of atomic force microscopy.

Poly-carbonate was selected as the subject of our investigation thanks to the bio-compatibility and solubility in non-dangerous solvents of this polymer. Further studies are in progress in order to describe the effect of the UV laser based surface structuring on the topographical, chemical and adhesion properties of poly-styrene, which is the most frequently used polymer in bio-medicine.

Acknowledgements

Financial support of this research was provided by the SFB Grant Nr. 1815, and the Hungarian Foundations: OTKA No. T34825, TS040759 and M41862. M. Csete would like to thank for the OTKA Hungarian post-doc fellowship D42228 and for the János Bolyai Research Scholarship of the Hungarian Academy of Sciences. We gratefully acknowledge the many discussions with S. Hild, N. Maghelli and A. Schmatulla.

References

- [1] E.K.F. Yim, R.M. Reano, S.W. Pang, A.F. Yee, C.S. Chen, K.W. Leong, *Biomaterials* 26 (2005) 5405.
- [2] M. Otto, B. Wahn, C.J. Kirkpatrick, *J. Mater. Sci./Mat. Sci. Med.* 14 (2003) 263.
- [3] P. Mitchell, *Nat. Biotechnol.* 20/3 (2002) 225.
- [4] Y.B. Gerbig, A.R. Phani, H. Haefke, *Appl. Surf. Sci.* 242 (2005) 251.
- [5] G.V. Lubarsky, M.R. Davidson, R.H. Bradley, *Surf. Sci.* 558 (2004) 135.
- [6] M. Nowicki, A. Richter, B. Wolf, H. Kaczmarek, *Polymer* 44 (2003) 6599.
- [7] M. Csete, J. Kokavecz, Zs. Bor, O. Marti, *Mater. Sci. Eng., C, Biomim. Mater., Sens. Syst.* 23 (2003) 939.
- [8] M.M. Browne, G.V. Lubarsky, M.R. Davidson, R.H. Bradley, *Surf. Sci.* 553 (2004) 155.
- [9] M. Csete, *Zs. Bor, Appl. Surf. Sci.* 133 (1998) 5.
- [10] C. Daniel, F. Mücklich, Z. Liu, *Appl. Surf. Sci.* 208–209 (2003) 317.
- [11] T. Voss, D. Scheel, W. Schade, *Appl. Phys., B* 73 (2001) 105.
- [12] H.M. Phillips, D.L. Callahan, R. Sauerbrey, G. Szabó, Z. Bor, *Appl. Phys. Lett.* 58 (24) (1991) 2761.
- [13] A. Rosa-Zeiser, E. Weilandt, S. Hild, O. Marti, *Meas. Sci. Technol.* 8 (1997) 1333.
- [14] J.E. Sader, J.W.M. Chon, P. Mulvaney, *Rev. Sci. Instrum.* 70/10 (1999) 3967.
- [15] A. Mechler, J. Kokavecz, P. Heszler, R. Lal, *Appl. Phys. Lett.* 82 (2003) 3740.
- [16] M. Stark, C. Möller, D.J. Müller, R. Guckenberger, *Biophys. J.* 80 (2001) 3009.
- [17] B.V. Derjaguin, V.M. Muller, Yu. P. Toporov, *J. Colloid Interface Sci.* 53 (1978) 378.